CTAU, A Cartesian Grid Method for Accurate Simulation of Compressible Flows with Convected Vortices

Philip Kelleners and Frank Spiering

Abstract A zonal approach for simulation of compressible fluid flow is presented. Within this approach a Cartesian solver of fourth order spatial accuracy is used for simulation of convection of vortical structures over larger distances with small numerical losses.

1 Accurate Flow Simulation Using a Zonal Approach

Many present day well established aerospace numerical codes, of which the DLR TAU-code is an example, for the simulation of subsonic, transonic or supersonic flow are second order accurate in physical space. For these second order codes it has been observed that freely convecting vortices, amongst other free convected coherent structures, suffer from rapid decay on grids of practical mesh density. The computational cost of accurate simulation of freely convected vortices becomes rapidly excessive as the distances over which the vortices travel increase, for second order accurate codes. Presently designated higher-order methods, that is of spatial order higher than two, are better able to represent these free vortices on grids of moderate density, and thus potentially, could lower the computational cost. However these higher-order methods may not be well suited to simulate flows with discontinuities like strong shocks in transonic flow, or close to complex shaped solid structures embedded in the fluid. A solution is a zonal approach. Within this zonal approach, based on experience, that is best-practice, the flow domain of interest is simulated with different discretization methods each being applied in those regions where their strengths excel. In the implementation of this zonal approach developed and presented here the boundaries of the different grids overlap and the developing flow

P. Kelleners (✉) · F. Spiering
DLR, Institute of Aerodynamics and Flow Technology, Lilienthalplatz 7,
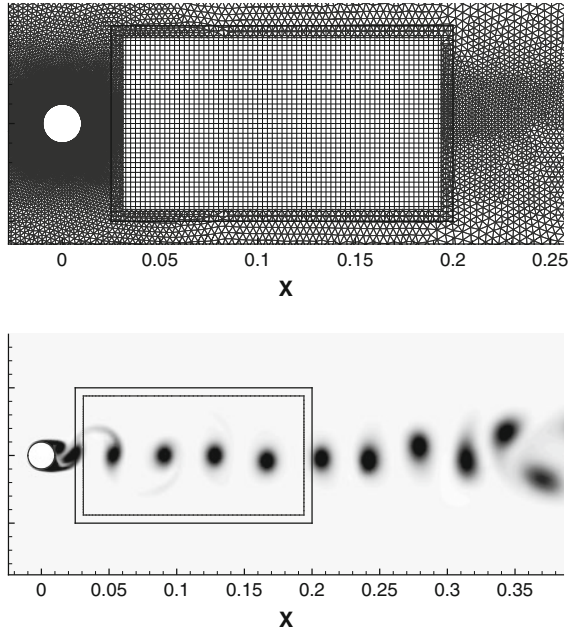38108 Braunschweig, Germany
e-mail: Philip.Kelleners@dlr.de

Fig. 1 The von Kármán vortex street behind a circle cylinder. A closeup of the chimera grid in the upper part, dimensionless entropy-like quantity given by the greyfilled iso-contours in the lower part

state is coupled in these overlapping regions. This procedure is called the Chimera or overset grid approach, and the overlapping grids are also referred to as Chimera grids (see [1]). This zonal approach is illustrated in Fig. 1. The DLR TAU-code, a second order accurate method is used for the regions of the flow close to the solid geometry. CTAU, the Cartesian grid higher order method presented here, is used on the portion of the grid enclosed by the two boxes. As can be seen from the thick black lines, the grids overlap at their boundaries where a code coupling module, (see [2]), performs the exchange of the fluid states and thus implements a strong volume coupling based upon the Chimera technique. The two components of this framework other than the Cartesian Solver are presented briefly below.

1.1 TAU Code

The DLR TAU-code is a fully featured package for simulation of steady and unsteady flow, of both inviscid and viscous compressible fluids, on unstructured hybrid, possibly moving, grids. It implements different turbulence models, overset grid techniques (Chimera), a large number of physical boundary conditions and can efficiently compute solutions on massive parallel computer clusters; e.g. see [3].

1.2 Code2Code Domain Coupling

The Code2Code program (see [2]) is the domain coupling tool, implementing a Chimera boundary between two possibly different CFD-codes, designated code A and code B. The domain coupling is done in three basic steps. There must be a region where the grid domain boundaries of code A and code B overlap. The coefficients for the data-exchange and interpolation for the overlapping region of grids A and B must be computed. At Run-time there must be exchange of the flow-states at the domain boundary grid overlap area at every time level or relaxation step. Code A and code B can be any different code or two instances of the same code.

2 Cartesian Solver, CTAU

The Cartesian solver prototype CTAU is a derivative of the TAU-code. It is a conventional explicit Runge–Kutta based relaxation solver for steady or unsteady flow problems. Discretization of the spatial terms in the equations of fluid flow is done using compact finite difference schemes, or Padé-type schemes, (see [4]), which formally, can be up to tenth order accuracy in space when operating on Cartesian meshes.

2.1 Padé Schemes

As a quick way to illustrate these compact finite difference schemes consider values u_i of a function given at discrete nodes on a regular equidistant one dimensional mesh. Quantities constructed from these nodal values like the derivative u'_i or interpolated values, $u_{1/2}$ inbetween the discrete nodes are computed by *implicit* operators with difference molecules of limited footprint. As an example a first derivative of fourth order accuracy is:

$$u'_{i-1} + 4u'_i + u'_{i+1} = \frac{3(u_{i+1} - u_{i-1})}{h}, \tag{1}$$

where index i designates the position on the regular mesh, u' is the first derivative of u and h is the local meshspacing. The expression for interpolation is:

$$u_{i-1/2} + 6u_{i+1/2} + u_{i+3/2} = 4(u_i + u_{i+1}), \tag{2}$$

which is also fourth order accurate. Inspect the left hand sides of (1) and (2) to check that the derivative or the interpolated values are given in implicit form. For these examples the actual values of the derived or interpolated quantities, at fourth order accuracy, comes at the price of having to solve a tridiagonal system of equations.

In the paper of [4] implicit formulations of up to tenth order accuracy of these Padé operators are given of the general form;

$$\beta u'_{i-2} + \alpha u'_{i-1} + u'_i + \alpha u'_{i+1} + \beta u'_{i+2} = a\frac{u_{i+1} - u_{i-1}}{2h} + b\frac{u_{i+2} - u_{i-2}}{4h} + c\frac{u_{i+3} - u_{i-3}}{6h},$$

(3)

where the parameters α, β, a, b and c are derived by matching Taylor series coefficients of various orders. Different schemes of different order of accuracy can be derived for particular combinations of these parameters, again the reader is referred to [4].

2.2 Padé-type Operators for Finite Volume Schemes

The implicit operators introduced above are used in a finite difference context. For the simulation of fluid flow, the conservation properties of the numerical scheme used are of prime importance. Finite-volume schemes are inherently conservative whereas finite difference schemes are not. A finite-volume formulation of the Padé-type scheme, as described by Lacor et al. [5], which restores conservation of the dependent, now cell averaged, quantities is implemented in the Cartesian solver presented. The basis for the finite-volume formulation is the definition of *cell-averaged* dependent variables or quantities:

$$\bar{u}_i \equiv \frac{1}{(x_{i+1/2} - x_{i-1/2})} \int_{x_{i-1/2}}^{x_{i+1/2}} u(\xi)d\xi.$$

(4)

The fourth order accurate Padé-type operators used as examples before are now expressed in the cell averaged quantity $\bar{u}_i$:

$$u'_{i-1} + 4u'_i + u'_{i+1} = \frac{3(\bar{u}_{i+1} - \bar{u}_{i-1})}{h},$$

(5)

for the first derivative, and:

$$u_{i-1/2} + 4u_{i+1/2} + u_{i+3/2} = 3(\bar{u}_i + \bar{u}_{i+1}),$$

(6)

for the interpolated values.

Notice how the stencil weights for the interpolated values have changed as a result of application of cell averaged values.

We are concerned with fluid flow. With the finite volume method we need to calculate the fluxes at the interfaces of the control volumes, hence the emphasis on the ability to calculate interpolated values. The fluxes of the Euler and Navier-Stokes equations of motion of fluid are non-linear, as illustrated by a line integral in y-direction for the mass flux in x-direction for two dimensional flow:

$$\int_a^b \rho(x, y)u(x, y)dy, \tag{7}$$

which complicates matters considerably as products of the primitive values are not readily available at the volume interfaces. A second order accurate approximation for the flux, averaged over the interface, is:

$$\frac{1}{y_b - y_a} \int_a^b \rho u dy \approx \frac{1}{y_b - y_a} \int_a^b \rho dy \, \frac{1}{y_b - y_a} \int_a^b u dy. \tag{8}$$

Additional correction terms of the form $\rho'_x u'_x \frac{\Delta x^2}{12}$ are needed to compute a fourth order accurate flux, where the first derivatives are now evaluated at the interfaces, for the details again refer to [5].

Ghost cells opposite of the domain boundary with quasi cell-averaged values prescribed by the local physical character at the boundary are needed to complete the boundary fluxes.

An implicit assumption for these Padé-type schemes is that argument values and their derivatives exist and are continuous. This is generally not true for discrete initial data, boundary conditions or when flow conditions result in flow structures like e.g. shear regions at length scales which are not resolved by the grid. As a result spurious waves will become part of the discrete solution. These spurious waves are removed effectively from the solution by high-order Padé filters, designed with similar discretization techniques as used for computation of the derivatives, to filter the solution to restore monotone solutions.

To limit the complexity of the current implementation of the Cartesian solver only the Padé-type schemes with parameter β set to zero are considered such that only tridiagonal systems of coupled equations need to be solved. As a consequence the complexity of implementation of the boundary conditions in the ghost cells is reduced.

2.3 Gust Boundary Condition

A series of boundary conditions is available in the Cartesian Solver e.g. farfield and symmetry boundary conditions as well periodic boundaries. The domain coupling interface as introduced in Sect. 1.2 is also implemented as a boundary condition.

To be able to accurate simulate aircraft response due to gust loading while there is a strong interaction between the aircraft structure, aircraft induced flow patterns and the gust itself is one of the goals of this research and development. Preferably the gust enters the flow domain at the farfield, is transported towards the aircraft, interacts with the aircraft and leaves the domain again at the farfield. The discrete gust should suffer much less from dissipation and dispersion errors as it is convected over large distance from the farfield towards the aircraft by the Cartesian solver.

A gust boundary condition at the farfield is superimposed on a non-reflecting inflow boundary condition. The gust is modeled as a velocity profile perpendicular to the undisturbed mean flow u_∞:

$$v = v(x, t) = v(x - u_\infty t), \tag{9}$$

with pressure and density, and thus internal energy as well, taken constant at inflow. This gust-model is a solution to the Euler equations as can be checked by substitution.

The non-reflecting inflow boundary condition for subsonic flow is formulated by assuming local one dimensional inviscid flow, followed by an eigenvalue-eigenvector-analysis of the Euler equations, diagonalization of the system by pre-multiplication with the left eigenvectors, and identification of the waves entering the domain. These inward running waves are then replaced with physical boundary conditions simulating constant entropy and enthalpy (refer to [6] for more details). This gives:

$$\boldsymbol{l}_i^T \left(\frac{\partial \phi}{\partial t} + \lambda_i \frac{\partial \phi}{\partial x} \right) = -\boldsymbol{l}_i^T \boldsymbol{D}_{GH}$$
$$\boldsymbol{b}_j^T \frac{\partial \phi}{\partial t} = 0, \tag{10}$$

for i outward running characteristics and j inward running characteristics replaced with the boundary conditions $\boldsymbol{b}_j^T$. Notice that these boundary conditions have effective zero wave speed, $\lambda = 0$, thus are constant.

Then the actual $(1 - \cos)$-gust velocity profile superimposed at the inflow is formulated as a non-constant boundary condition:

$$\rho_\infty \frac{\partial v}{\partial t} = \rho_\infty \frac{2\pi}{L_{vg}} a_{vg} u_\infty^2 \sin \left(-\frac{2\pi}{L_{vg}} (x_\infty - x_{g0} - u_\infty t) \right), \tag{11}$$

with L_{vg} being gust length, a_{vg} the gust amplitude as dimensionless fraction of the undisturbed flow velocity u_∞, x_∞ the geometrical position of the farfield boundary and x_{g0} the initial position of the gust at time $t = 0$ beyond the farfield boundary. A result of a numerical experiment with this gust inflow boundary condition is shown in Fig. 2. Only minute spurious waves in the pressure, density were observed as the gust entered the domain. These numerical waves can be expected as the implementation of the discrete boundary condition is of a lower order of accuracy. However the typical dimensionless absolute error in the density induced by this boundary condition remained below $3 \cdot 10^{-4}$ at all simulated time.
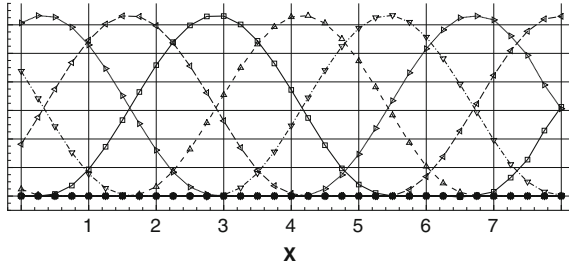
Fig. 2 Gust boundary condition; A domain of length 8, discretized with 32 cells. Flow from left to right. A $(1 - \cos)$-gust of length 5 is fed into the domain at the left inflow boundary. Shown with different linetypes is the position of the gust at regular time intervals. Note the near-perfect conservation of amplitude and shape of the gust as it is convected through the domain by the Cartesian solver

3 Testcases

3.1 Von Kármán Vortex Street Behind Circle Cylinder

The well known von Kármán vortex street is simulated at a free-stream Mach number of 0.1 at a Reynolds-number of 1,000. Both grid and a snapshot at a point in time where the vortex street is well developed are depicted in Fig. 1, the thick black boxes indicate the boundaries of the overlapping grids. The TAU-grid is hybrid with a prismatic layer wrapped around the circle cylinder for good support of the viscous boundary layer and the flow separation at the downstream side close to the cylinder. The vortices are convected with very small losses over the full length of the Cartesian domain, whereas they are quickly dissipated upon further convection in the triangular TAU-grid.

3.2 Wake Flow Resulting from Transonic Buffet

The configuration of the two airfoils shown in Fig. 3 is a useful approximation to study the effect of the unsteady wake, resulting from transonic wing buffet, as it interacts with a horizontal tailplane. The wing is modeled with the supercritical NLR7301 airfoil of 4.47 m length at an angle of incidence of 3°. The horizontal tailplane is modeled with a NACA0012 airfoil of half the wing-chord length at 0° angle of incidence. The undisturbed flow is angled at 0.5°, freestream Mach number is 0.73 and the Reynolds number is 26 million. At these conditions shock buffet occurs over the wing airfoil and the unsteady wake influences the pressure distribution at the tailplane considerably. Development in the wake of structures of considerable size in the crossflow direction could only be observed in simulations performed with the Cartesian solver inbetween the two airfoils.
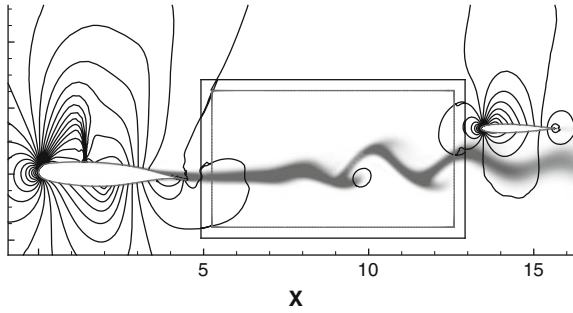
Fig. 3 A snapshot of flow at conditions of transonic buffet; the wake of the wing airfoil interacting with a tailplane airfoil. Greycolored isocontours depict a dimensionless entropy-like quantity, the static pressure is drawn with black isolines, the black boxes show the overlapping boundaries of the chimera grid parts
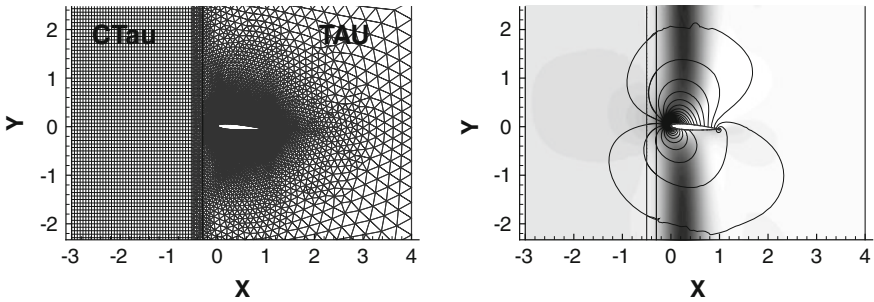

Fig. 4 Gust encounter, grid on the left, vertical velocity (isocontours) and pressure (black iso-lines) on the right at the moment in time of maximum lift during the gust encounter

3.3 Gust Encounter, NACA0012

The gust-velocity model described in Sect. 2.3 is convected in a Cartesian grid shown to the left in Fig. 4, towards a NACA0012 airfoil fixed in space at 4° angle of attack at a freestream Mach-number of 0.3. The gust length is 1.4 times the chord length of the airfoil, the gust amplitude fraction, a_{vg}, is $\frac{1}{8}$th of the undisturbed freestream velocity. The flow is inviscid. There is no noticeable decay of the gust as it is transported in the Cartesian grid and it interacts in its unaltered shape with the airfoil as intended. At the moment of maximum lift, as shown in the figure, the lift coefficient (C_l) peaks at approximately 2.5 times the value of lift generated in steady undisturbed flow. After having traversed along the fixed airfoil, the structure of the gust has changed significantly and it was observed that inside the airfoil wake the downflow induced by the airfoil is dominant. We conclude that the zonal approach enables near lossless gust convection and accurate gust-airfoil interaction.

4 Conclusions

A zonal approach for simulation of compressible fluid flow has been presented. The Padé-type scheme used in a finite volume context to simulate flow of a compressible, possibly viscous, fluid at fourth order accuracy on Cartesian grids has been introduced, as well as a gust-velocity boundary condition superimposed upon a non-reflective inflow boundary condition. Three testcases showing the effective use of the higher order Cartesian method with help of chimera-based domain coupling between two different flow solvers, illustrate the prosperous perspective of the present framework under development. Further work will include testing of the method on full three dimensional configurations and, amongst others, implementation of whirl fluxes to allow for moving meshes, as needed for simulation of rotorcraft.

References

1. Chesshire, G., Henshaw, W.D.: Composite overlapping meshes for the solution of partial differential equations. J. Comp. Phys. **90**, 1–64 (1990)
2. Spiering, F.: Coupling of TAU and TRACE for parallel accurate flow simulations. In: International Symposium "Simulation of Wing and Nacelle Stall", Braunschweig Germany, June 2012
3. Schwamborn, D., Gerhold, T., Heinrich, R.: The DLR TAU-code: recent applications in research and industry. Invited Lecture. In: Proceedings on CD of the European Conference on Computational Fluid Dynamics ECCOMAS CDF (2006).
4. Lele, S.K.: Compact finite difference schemes with spectral-like resolution. J. Comp. Phy. **103**, 16–42 (1992)
5. Lacor, C., Smirnov, S., Baelmans, M.: A finite volume formulation of compact central schemes on arbitrary structured grids. J. Comp. Phys. **198**, 535–566 (2004)
6. Kelleners, P. H.: An edge-based finite volume method for inviscid compressible flow with condensation. Ph.D. Thesis, University of Twente (2007)